

## Wave Activity on the Tropical Easterly Jet

S. E. NICHOLSON

*Department of Meteorology, The Florida State University, Tallahassee, Florida*

A. I. BARCILON

*MMM Visiting Scientist, NCAR, Boulder, Colorado*

M. CHALLA

*Geophysical Fluid Dynamics Institute, The Florida State University, Tallahassee, Florida*

J. BAUM

*Department of Meteorology, The Florida State University, Tallahassee, Florida*

(Manuscript received 19 September 2005, in final form 9 October 2006)

### ABSTRACT

This article examines the question of the existence of waves on the tropical easterly jet (TEJ) over West Africa. The TEJ is a well-known feature of the Asian monsoon and waves on the jet have been implicated in various weather phenomena. Its role in West African meteorology has received little attention. A model simulation of wet and dry years over West Africa predicted wave development on the TEJ. NCEP reanalysis data confirmed the existence of these waves, using case studies in the dry year 1983 and the wet year 1950. Both the simulated and observed waves are of planetary scale, with a period of 5–6 days. Potential vorticity (PV) theory suggests that they develop via interactions between the surface and the TEJ. Overall, the results suggest that interactions between the TEJ and African easterly jet play an important role in the development of wave disturbances over West Africa.

### 1. Introduction

The tropical easterly jet stream (TEJ) is one of the most intense circulation features over Africa. This jet lies in the upper troposphere and extends from Asia to West Africa, reaching core speeds in excess of  $35 \text{ m s}^{-1}$ . It spans some  $20^{\circ}$ – $30^{\circ}$  of latitude. Most research on the TEJ has been in the context of the Indian monsoon (Mishra 1987; Chen and Yen 1991, 1993; Chen and van Loon 1987). It is considered to be an active player in the monsoon system. Specifically, waves on the TEJ in the Asian sector have been shown to play a role in the growth and development of monsoon disturbances (Mishra and Salvekar 1980).

Over Africa the TEJ tends to be viewed as a passive system, despite the fact that the jet's intensity is one of the strongest contrasts between wet and dry years in West Africa (Kanamitsu and Krishnamurti 1978; Newell and Kidson 1984; Grist and Nicholson 2001). Much greater interest has been shown in the African easterly jet (AEJ), a weaker system with its core in the midtroposphere near 650 or 700 hPa (Thorncroft et al. 2003).

We have recently incorporated the TEJ into a modeling study of the dynamics of this region, following up on the work of Grist et al. (2002). In the current study, the model predicted the presence of waves on the TEJ over West Africa, a feature that to our knowledge has not been documented in the literature. We then examined National Centers for Environmental Prediction (NCEP) reanalysis data to determine whether or not the predicted waves could be observed during the time periods predicted by the model. This note reports on our findings.

---

*Corresponding author address:* S. E. Nicholson, Dept. of Meteorology, The Florida State University, Tallahassee, FL 32306.  
E-mail: sen@met.fsu.edu

## 2. Data and methodology

This study utilizes NCEP reanalysis data (Kalnay et al. 1996) to produce zonally averaged basic states for model simulations and to identify waves on the TEJ. The spatial resolution of the data is  $2.5^\circ$  latitude  $\times$   $2.5^\circ$  longitude. For the model's basic states, monthly means of wind and potential temperature are derived. Data are averaged for the region between  $10^\circ$ W and  $10^\circ$ E. Potential temperature from NCEP is used to estimate a stability parameter in the model. NCEP 6-hourly wind data are also used to determine if the predicted waves are actually observed.

The observational analysis is carried out in a simple fashion. Hovmoeller diagrams of meridional wind are produced from filtered NCEP wind data. A 62-point fast Fourier transform (FFT) bandpass filter was applied. The filter retains periodicities on the time scale of 2–6 days, the basic time scale of the African easterly waves (Adefolalu 1974; Burpee 1972). A comparison made with unfiltered data showed that the most important features in the analysis were also apparent in the unfiltered data. Streamlines are also shown for an individual wave on the TEJ that was linked to very high rainfall over Sahelian Africa.

The numerical simulations utilize a model provided by J. Whitaker of the National Oceanic and Atmospheric Administration Climate Diagnostics Center (NOAA/CDC; see Peng and Whitaker 1999). It is a nonlinear, spectral, and spherical primitive equation model but is here used as a linear GCM. The model, with triangular truncation at T32, contains 32 waves and has  $48 \times 96$  horizontal grid points covering the entire globe. This results in a grid size of approximately  $3.7^\circ$  of latitude and longitude. The model has up to 20 levels in the vertical. Lateral sponge layers are imposed from  $38^\circ$  of latitude to the Poles on both sides of the equator at all levels. Further details of the model are found in Nicholson et al. (2006, manuscript submitted to *J. Atmos. Sci.*, hereafter NBC).

The simulations are initial value experiments that use a weak barotropic Gaussian vortex placed at  $17^\circ$ N,  $0^\circ$  to excite nonmodal perturbations. The vortex has a radius of 1500 km. The maximum zonal wind is  $9 \text{ m s}^{-1}$  at a radius of 700 km and outside the initial vortex the perturbations are zero. A zonal time-averaged basic state circumscribing the globe is constructed for different months and years. These are described in NBC.

The results presented here are for July only during a very wet year in the West African Sahel (1950) and a very dry year (1983). An analysis for August of these years was also carried out and yielded similar results. In this we are interested only in wave behavior over a

limited area, the some 5000 km of West Africa. For that reason, we examine the waves at day 6 of the linear integration, roughly corresponding to a distance of 5000 km. By this time, the wave characteristics had stabilized and in the wet years exponential growth had begun.

## 3. Numerical simulation results

In Fig. 1, the zonal distribution of the streamfunction after the 6-day integration is plotted as a function of pressure and longitude for July 1950 (right panel) and July 1983 (left panel). The latitudes depicted in the picture are  $17^\circ$ N, the Sahelian latitude where the vortex was introduced, and  $13^\circ$ N, in the southern Sahel. The indicated longitudes are degrees east or west of the initial perturbation and do not correspond to geographical longitude.

Waves are clearly present at TEJ level (150–300 hPa) at  $17^\circ$  and  $13^\circ$ N. The resulting perturbations at the TEJ level have longer wavelengths than those in the midtroposphere at the level of the AEJ and surface waves. Figure 1 also suggests numerous contrasts between waves in the dry year (1983) and the wet year (1950). For example, in the wet year the waves at the TEJ level are very strong and lie ahead of the largest waves at the AEJ and surface levels. The waves originate at the AEJ level and propagate upward to the TEJ level. This suggests interaction between the TEJ and AEJ. In the dry year, the upper-level waves are weaker and aligned with the AEJ and surface waves. The waves are strongly suppressed above 500 hPa in 1983. Also, the waves appear to be barotropic in 1983 but slightly baroclinic in 1950, at least in the mid- and lower troposphere. Another contrast to note is the westward displacement of the TEJ waves with respect to the initial vortex in the wet year, but not in the dry year. This is consistent with the difference in the speed of the TEJ in these 2 yr.

The model's waves on the TEJ were determined to be wave -5 or -6 planetary waves. By comparison, Mishra (1993) and Kanamitsu et al. (1972) found wave -6 in model simulations and observations of the TEJ over India. In contrast, the disturbances evident at 625 hPa near the AEJ are synoptic in scale, with horizontal scales of 3000–4000 km (i.e., much smaller than the planetary-scale waves evident at 125 hPa).

Figure 2 provides a spatial picture of the waves on day 6 and a direct comparison of the lower, mid-, and upper troposphere in the wet and dry years in areas well beyond the Sahel. The 875-, 625-, 375-, and 125-hPa pressure surfaces are depicted. A major contrast between these years is the latitudinal location of the wave maximum and the latitudinal extent of the waves.

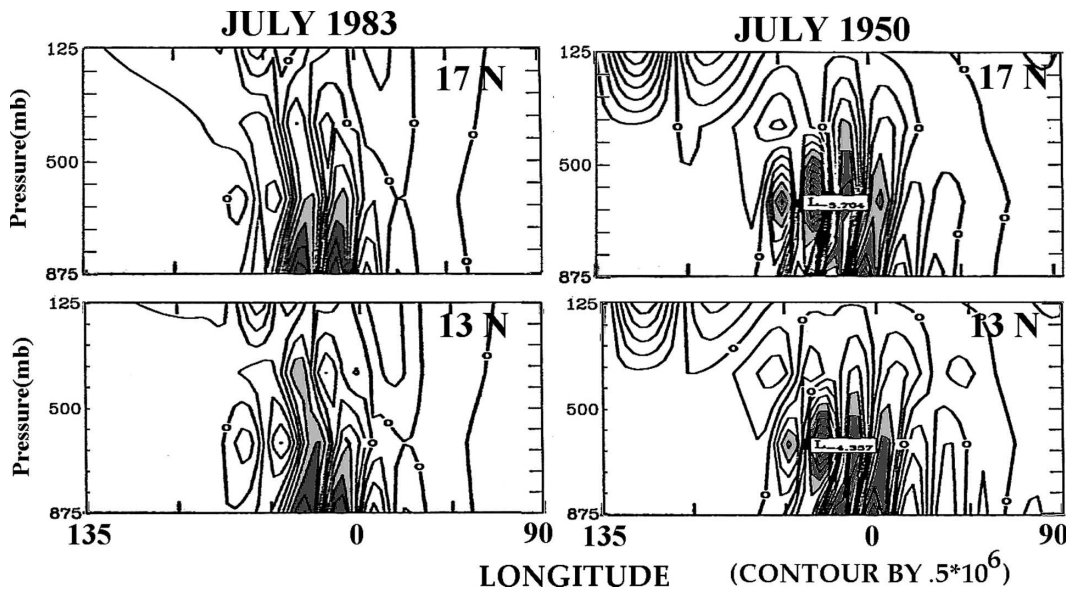


FIG. 1. Pressure-longitude section of the waves, expressed as the perturbation streamfunction ( $10^{-6} \text{ m}^2 \text{ s}^{-1}$ ) at  $13^\circ$  and  $17^\circ\text{N}$  as a function of longitude and pressure after 6-day integration for (left) July 1983 and (right) July 1950. Longitude represents degrees east or west of the location where the initial vortex was introduced into the basic state. Contours are at intervals of 0.5. The light shading indicates values between 1.5 and 2.0 and the dark shading is for values exceeding 2.0.

At the TEJ level (125 hPa), strong waves are apparent in both years. In the wet year the maximum lies near or beyond  $20^\circ\text{N}$  latitude. The waves are well developed in the Sahelian latitudes. In the dry year the strongest TEJ waves are over the equator and they extend well into the Southern Hemisphere. The TEJ waves are weak north of  $15^\circ\text{N}$  and hence were not apparent in Fig. 1. The TEJ waves are also weaker in 1983 than in 1950, but several waves are present. In 1950, a single explosive wave is evident and it is clearly confined to the Northern Hemisphere. There is less contrast between the 2 yr in the mid- and lower troposphere, at 625 hPa and 875 hPa. The wave maximum lies in the Sahelian latitudes around  $20^\circ\text{N}$  during the wet year but near the equator in the dry year. Also at 625 hPa the waves are stronger in the wet year and confined to a smaller latitudinal span.

At 375 hPa, an interesting feature emerges in both years: a U-shaped, fairly intense wave packet. In the wet year the lower branch of the U is over the equator and the upper branch lies farther north, in the latitudes where the TEJ waves are found. The wave maximum at 375 hPa lies in the Northern Hemisphere. In the dry year, the upper branch of the U is very weak and it lies near the equator. The much stronger lower branch penetrates deeply into the Southern Hemisphere. The development of packets suggests a broad range of unstable wavelengths, consistent with the growth rates predicted by the model in the wet and dry years (NBC).

#### 4. Observational results

Figure 3 shows Hovmoeller diagrams of filtered meridional wind at  $10^\circ\text{E}$ , averaged for latitudes  $12.5^\circ$ – $20^\circ\text{N}$ . These latitudes represent the expanse of the Sahel. Waves are definitely present at the TEJ level (200–100 hPa) in both July 1950 (Fig. 3a) and July 1983 (Fig. 3b). Although the data presented are filtered to emphasize 2–6-day variability, the waves are evident in the unfiltered data as well.

As predicted by the model, during the dry year the waves are generally weak at the AEJ level (650–700 hPa) but well developed in the upper troposphere. The TEJ waves appear to be barotropic in the dry year (1983), but some baroclinic waves appear in the wet year (1950). In the wet year they are well developed at the AEJ level and reasonably strong at the TEJ level. This is likewise consistent with model results. The observations also confirm the longer waves at the TEJ level rather than the AEJ level, as predicted by the model. In both 1983 and 1950, the waves have a period of roughly 5–6 days at the TEJ level, compared to 3 or 4 days at the AEJ level.

Figure 4 shows the filtered wind data at 150 hPa, the level at which the TEJ is generally best developed. This figure emphasizes the number and intensity of the waves in the two years. The 5–6-day period of the waves is clearly apparent in both years. There is, however, a difference in intensity in these years. In 1950 only three

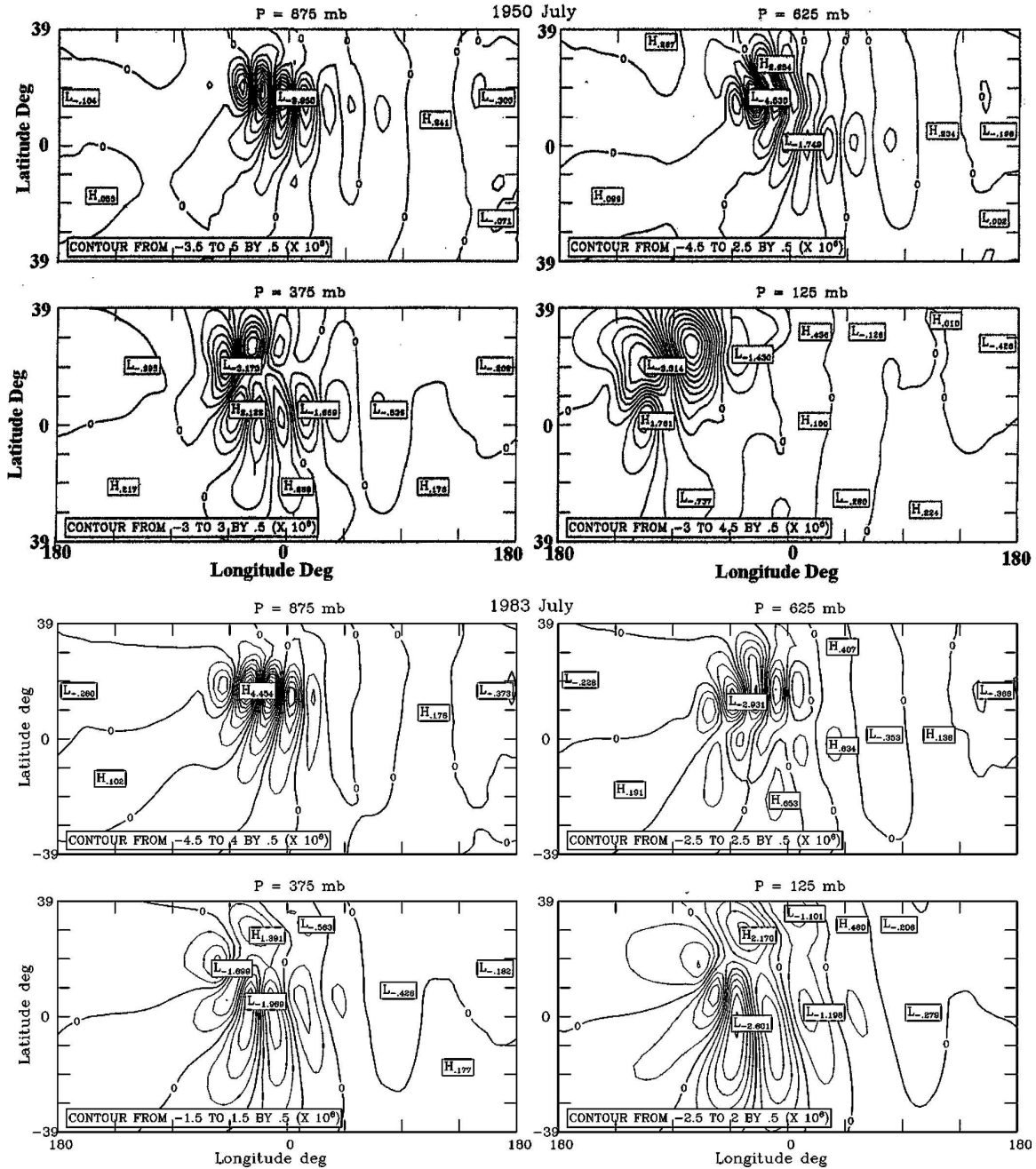


FIG. 2. Horizontal distribution of perturbation streamfunction ( $m^2 s^{-1}$ ) at four pressure levels after 6-day integration for July (top) 1950 and (bottom) 1983. Amplitude is represented by the difference between maximum and minimum values of the streamfunction.

waves exceed  $1 m s^{-1}$ , but in 1983 five waves exceed  $1 m s^{-1}$  and three exceed  $1.5 m s^{-1}$ . The speed differential between crest and trough is also clearly greater in 1983. Thus, the waves are generally weaker in 1950 at the TEJ level. However, there is one exceedingly strong wave at this level in 1950. This is consistent with the model results, which showed several well-developed waves in 1983 but one very strong wave in 1950.

Streamlines clearly show the wave indicated in Figs. 3, 4 on 25 July 1950. The TEJ wave was best developed at 200 hPa. The situation became interesting as the wave moved westward. By 27 July (Figs. 5, 6), it was centered near  $10^{\circ}W$  and was associated with a cyclonic center at 1000 hPa and a wave in the AEJ at 600 hPa (not shown). Both reanalysis and gauge data show that this system was associated with heavy rain in southern

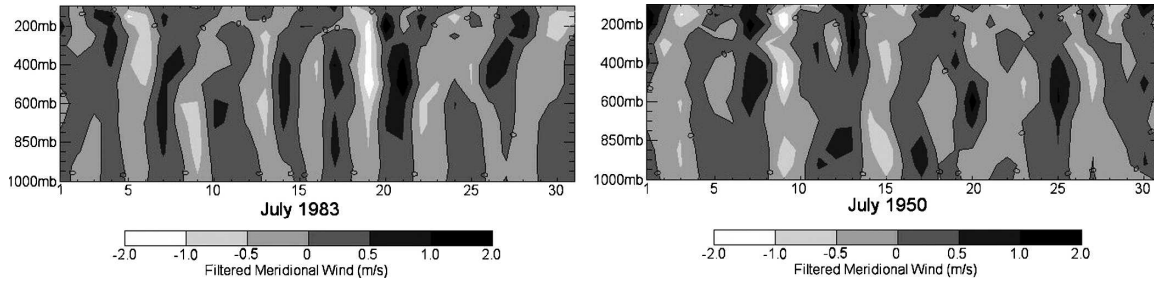


FIG. 3. Hovmoeller diagrams of filtered meridional wind at  $10^{\circ}\text{E}$  for July 1983 and 1950 (averaged for  $12.5^{\circ}\text{--}20^{\circ}\text{N}$ ).

Mali, Guinea, and the northern Ivory Coast. At Dioila, Mali ( $12^{\circ}23'\text{N}$ ,  $6^{\circ}53'\text{W}$ ), 105 mm fell on 27 July. This is half of the monthly mean for that station.

As the wave moved farther west on 28 July (Fig. 7), it was still associated with a cyclonic center at 1000 hPa and a wave in the AEJ at 600 hPa. At 200 hPa, a closed circulation developed north of the TEJ wave and moved off the coast. This picture is remarkably like that shown in Fig. 1 for July 1950, with a closed circulation developing at 200 hPa north and west of the initial perturbation.

The synoptic situation shown in Fig. 7 is favorable for the development of tropical depressions over the Atlantic. A warm core system is marked by cyclonic circulation at low levels and anticyclonic circulation at high levels, but somewhat north and west of the low-level cyclone. In this particular case, the system developed far enough north that a westerly steering current took it eastward instead of westward. Nevertheless, the development of this situation from a wave in the TEJ suggests that the TEJ over Africa may play some role in hurricane formation.

## 5. Discussion and conclusions

The use of this simple model, in conjunction with observational analysis, provides us with insights be-

tween the TEJ, the AEJ, and baroclinic waves in the lower atmosphere as driven by latitudinal temperature gradients. The model prediction of waves on the TEJ over West Africa is validated by the observational analysis. The agreement between model and observational results is gratifying. Both model and observations show that the TEJ waves are better developed in the dry year and that the waves are planetary scale, in contrast to synoptic-scale waves on the AEJ.

A noteworthy model result is the extension of the waves on the TEJ into the Southern Hemisphere in the dry year and the limited latitudinal extent in the wet year. This is consistent with the zonal wind shear in the upper troposphere between the TEJ core and the equator (not shown). The shear is weak in the wet year but exceedingly strong in the dry year.

It is interesting to speculate on possible causes of waves of the TEJ over Africa. What immediately comes to mind is the possibility of a trigger via the Asian monsoon upstream or by a wave on the TEJ in the Asian region. This would hint at teleconnections between North Africa and the Asian monsoon. Recent papers have shown interesting teleconnections between the midlatitudes and the Tropics over the African/Asian sector that could also provide triggers for a TEJ wave (Rowell 2003; Ding and Wang 2005). The mid-latitude influence finds some support in the causes of

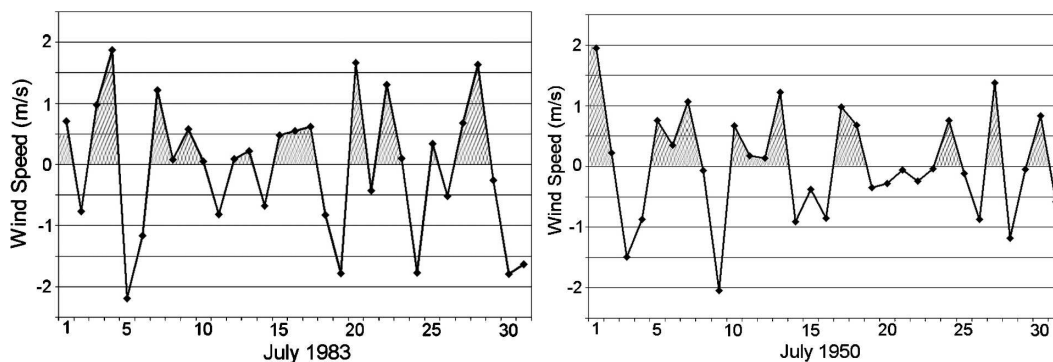


FIG. 4. Filtered meridional wind at 150 hPa, at  $10^{\circ}\text{E}$  for July 1983 and 1950 (averaged for  $12.5^{\circ}\text{--}20^{\circ}\text{N}$ ).

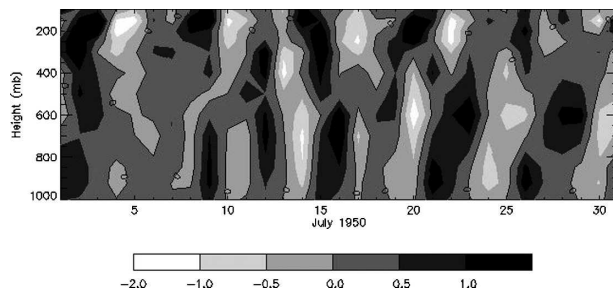


FIG. 5. Hovmoeller diagram of filtered meridional wind at  $10^{\circ}\text{W}$  for July 1950 (averaged for  $12.5^{\circ}$ – $20^{\circ}\text{N}$ ).

some wet years: an enhanced cross-equatorial pressure gradient that is imposed primarily by lower pressure over the extratropical latitudes of the central Sahara (Nicholson and Webster 2007, manuscript submitted to *Quart. J. Roy. Meteor. Soc.*).

Two other interesting features of the model results are the explosive growth on a single wave at the TEJ level in July 1950 and the vertical “cap” on waves at roughly the 400–500-hPa level (Fig. 1). Both features are probably related to the absence or reversal of the shear in the layer between 375 and 625 hPa. The shear reverses strongly in 1983, strongly limiting the vertical propagation of the waves. In 1950, the vertical shear is weak or absent. This probably hinders the vertical propagation (but not as effectively as in 1983), allowing only the strongest waves to reach the upper troposphere. In the strong shear above 375 hPa, the wave experiences strong baroclinic instability and explosive growth (see Fig. 2). This is particularly interesting in light of observations showing that the contrast between wet and dry years can be accounted for by only one or two large disturbances per month (Lamb et al. 1998; Nicholson 2000).

Perhaps the most significant result is the minimal wave activity at the AEJ level in the dry year and the maximum at this level in the wet year. This result is consistent with the observational results of Grist (2002), showing weaker wave activity in the dry years than in the wet years. This may provide the key to the contrast in rainfall in the 2 yr.

It is interesting to interpret the model results in the context of potential vorticity (PV) theory. In the situation we are simulating, there are essentially three PV reservoirs (i.e., dominant PV “lumps”): the ground, the AEJ, and the TEJ. The surface is involved because surface temperature plays the same role as PV. Each reservoir supports the propagation of PV waves (Barcilon and Bishop 1998). Wave communication exists between each pair of reservoirs when the “penetration” depth of the wave exceeds the vertical distance between the two

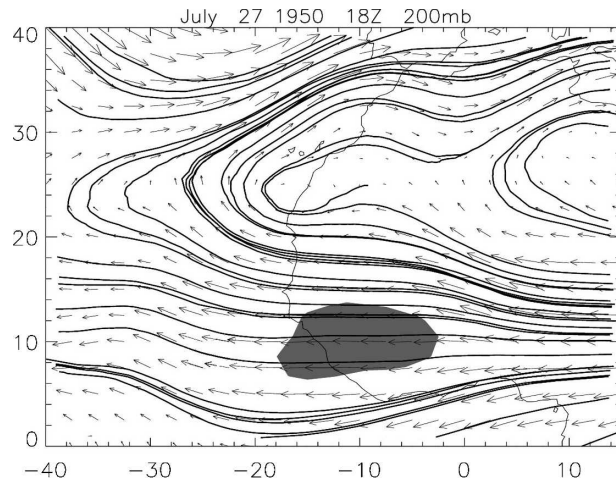


FIG. 6. Streamlines at 1800 UTC on 27 July at 200 hPa. Shading indicates the approximate region of heavy rainfall.

reservoirs (Bretherton 1966a,b). The vertical distance between the surface and the TEJ (tropopause) level is associated with planetary-scale waves. The comparable vertical distances between the surface and AEJ and between the AEJ and TEJ are associated with synoptic-scale waves.

It is tempting to utilize PV theory to speculate on the interactions between the TEJ and the other two “reservoirs.” One interpretation of the synoptic scale of the waves at the AEJ level is that they are triggered by interactions with the TEJ as well as interactions with the ground PV reservoir. There is some indication that this does, in fact, happen in 1983; the waves appear to begin at the TEJ level and propagate downward. In the wet year, the waves are clearly initiated lower in the atmosphere and eventually propagate upward to the TEJ level as they move westward. The result is the explosive growth of a planetary-scale wave on the TEJ.

This scale is consistent with surface–TEJ interaction and a possible interpretation is that the surface changes produced by rainfall associated with the AEJ waves help to trigger the TEJ wave. Examples are diabatic processes, such as increased baroclinicity, when the rainfall enhances the gradient between the desert and the Sahel and surface evaporation produces an additional source of moisture/latent heat. Further, it is interesting to note that the planetary-scale waves are evident in the wet year but not the dry, a finding confirmed for other years and months in NBC. In the dry years, stable air overrides the heat low of the western Sahara where the large temperature gradient exists. However, in the wet years (Fig. 8), this circulation is coupled with that associated with the AEJ (Nicholson 2007). This creates the surface–upper-tropospheric connection

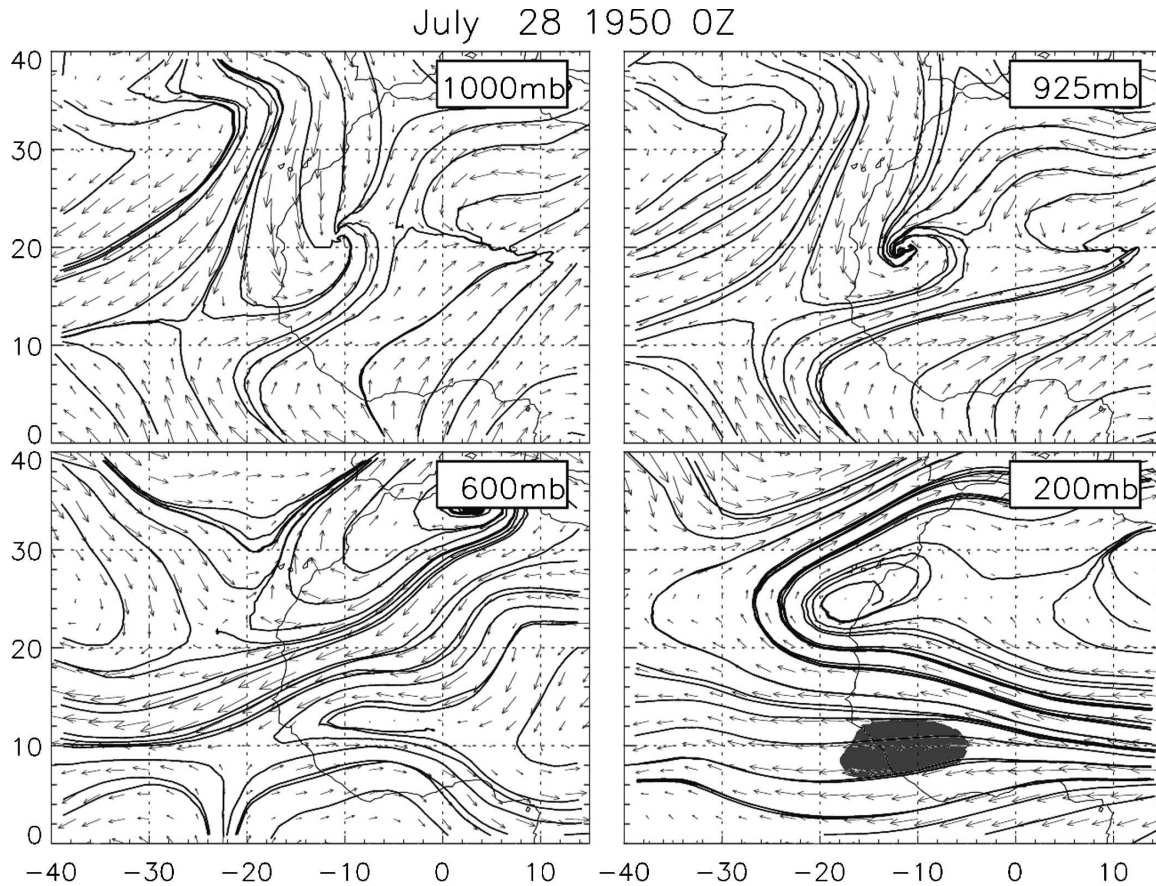


FIG. 7. Streamlines at 0000 UTC on 28 July at (a) 1000, (b) 925, (c) 600, and (d) 200 hPa.

required for the development of a planetary-scale wave.

The overbearing question, of course, is what triggers the waves at the AEJ level, since these are associated with squall lines and rainfall in the Sahel. Triggering by

waves at the TEJ level is not only theoretically possible, but a look at wave growth in the model beyond day 6 suggests that it does, in fact, occur during the wet year. Overall our results suggest that the planetary waves will contribute to the overall wave dynamics near the AEJ.

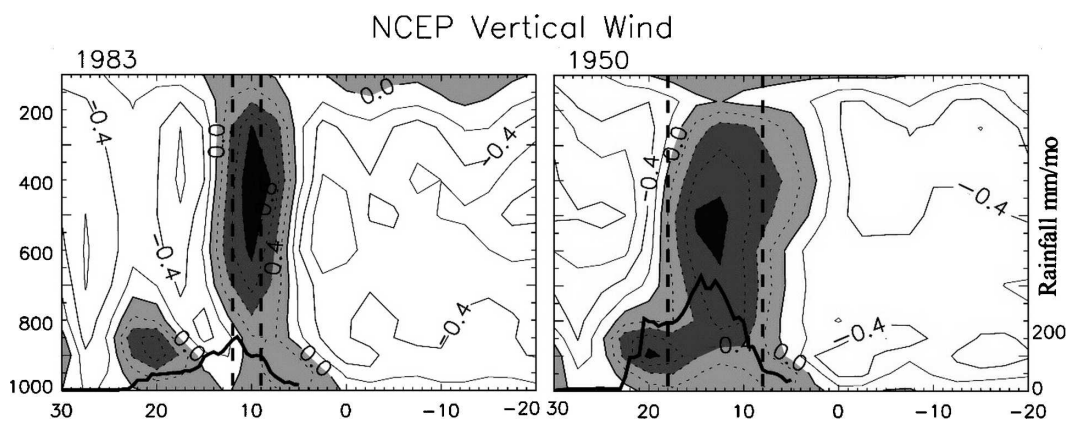


FIG. 8. Vertical cross section of  $\omega$  ( $\text{m s}^{-1}$ ) in July 1983 and 1950. Axes of the AEJ and TEJ are superimposed, respectively, to the left and right of the column of strong vertical motion. Rainfall ( $\text{mm month}^{-1}$ ) as a function of latitude is indicated as a solid line.

Thus, the TEJ may be a critical factor in the development of the rainy season and the overall climate in West Africa.

*Acknowledgments.* This work was supported by NSF Grant ATM-0004479. We are much indebted to Dr. Jeff Whitaker, NOAA/CDC, who provided the model used in this study, and to NCAR for providing the NCEP reanalysis data. We would like to acknowledge the support for this research provided by the Geophysical Fluid Dynamics Institute of the Florida State University (a contribution number will be assigned after publication). We are grateful for discussions of this work with Profs. Robert Hart and Phil Cunningham of FSU. The third author would like to express his gratitude to Dr. C. A. Clayson, director of the Institute, for her support. Finally, we thank two anonymous reviewers, whose comments added much to the manuscript.

#### REFERENCES

- Adefolalu, D. O., 1974: The lower atmospheric summer easterly perturbation in tropical West Africa. Ph.D. thesis, The Florida State University, 276 pp.
- Barcilon, A. I., and C. H. Bishop, 1998: Nonmodal development of baroclinic waves undergoing horizontal shear deformation. *J. Atmos. Sci.*, **55**, 3583–3597.
- Bretherton, F. P., 1966a: Critical layer instability in baroclinic flows. *Quart. J. Roy. Meteor. Soc.*, **92**, 325–334.
- , 1966b: Baroclinic instability and short wavelength cutoff, in terms of potential vorticity. *Quart. J. Roy. Meteor. Soc.*, **92**, 334–345.
- Burpee, R. W., 1972: The origin and structure of easterly waves in the lower troposphere. *J. Atmos. Sci.*, **29**, 77–90.
- Chen, T.-C., and H. van Loon, 1987: Interannual variation of the tropical easterly jet. *Mon. Wea. Rev.*, **115**, 1739–1759.
- , and M.-C. Yen, 1991: Intraseasonal variations of the tropical easterly jet during the 1979 northern summer. *Tellus*, **43A**, 213–225.
- , and —, 1993: The effect of planetary-scale divergent circulation on the interannual variation of the summertime stationary eddies: The tropical easterly jet. *Tellus*, **45A**, 15–27.
- Ding, W., and B. Wang, 2005: Circumglobal teleconnection in the Northern Hemisphere summer. *J. Climate*, **18**, 3483–3505.
- Grist, J. P., 2002: Easterly waves over Africa. Part I: The seasonal cycle and contrasts between wet and dry years. *Mon. Wea. Rev.*, **130**, 197–211.
- , and S. E. Nicholson, 2001: A study of the dynamic factors influencing the interannual variability of rainfall in the West African Sahel. *J. Climate*, **14**, 1337–1359.
- , —, and A. I. Barcilon, 2002: Easterly waves over Africa. Part II: Observed and modeled contrasts between wet and dry years. *Mon. Wea. Rev.*, **130**, 212–225.
- Kalnay, E., and Coauthors, 1996: The NCEP/NCAR 40-Year Reanalysis Project. *Bull. Amer. Meteor. Soc.*, **77**, 437–471.
- Kanamitsu, M., and T. N. Krishnamurti, 1978: Northern summer tropical circulations during drought and normal rainfall months. *Mon. Wea. Rev.*, **106**, 331–347.
- , —, and C. Depradine, 1972: On scale interactions in the tropics during northern summer. *J. Atmos. Sci.*, **29**, 698–706.
- Lamb, P. J., M. A. Bell, and J. D. Finch, 1998: Variability of Sahelian disturbance lines and rainfall during 1951–1987. *Water Resources Variability in Africa during the XXth Century*, E. Servat et al., Eds., IAHS, 19–26.
- Mishra, S. K., 1987: Linear barotropic instability of the tropical easterly jet on a sphere. *J. Atmos. Sci.*, **44**, 373–383.
- , 1993: Nonlinear barotropic instability of upper-tropospheric tropical easterly jet on the sphere. *J. Atmos. Sci.*, **50**, 3541–3552.
- , and P. S. Salvekar, 1980: Role of barotropic instability in the development of monsoon disturbances. *J. Atmos. Sci.*, **37**, 383–394.
- Newell, R. E., and J. W. Kidson, 1984: African mean wind changes between Sahelian wet and dry periods. *J. Climatol.*, **4**, 1–7.
- Nicholson, S. E., 2000: Land surface processes and Sahel climate. *Rev. Geophys.*, **38**, 117–139.
- , 2007: The intensity and structure of the tropical rainbelt over West Africa as a factor in interannual variability. *Int. J. Climatol.*, in press.
- , A. I. Barcilon, and M. Challa, 2006: An analysis of West African dynamics using a linearized GCM. *J. Atmos. Sci.*, submitted.
- Peng, S., and J. S. Whitaker, 1999: Mechanisms determining the atmospheric response to midlatitude SST anomalies. *J. Climate*, **12**, 1393–1408.
- Rowell, D. P., 2003: The impact of Mediterranean SSTs on the Sahelian rainfall season. *J. Climate*, **16**, 849–862.
- Thorncroft, C. D., and Coauthors, 2003: The JET2000 Project: Aircraft observations of the African easterly jet and African easterly waves. *Bull. Amer. Meteor. Soc.*, **84**, 337–351.